

Sprayable Hydrogel for Instant Sealing of Vascular Anastomosis

Gonzalo Muñoz Taboada, Pere Dosta, Elazer R. Edelman, and Natalie Artzi*

Bleeding-related complications following vascular surgeries occur in up to half of the patients—500 000 cases annually in the United States alone. This results in additional procedures, increased mortality rate, and prolonged hospitalization, posing a burden on the healthcare system. Commercially available materials rely, in large, on forming covalent bonds between the tissue and the biomaterial to achieve adhesion. Here, it is shown that a biomaterial based on oxidized alginate and oxidized dextran together with polyamidoamine (PAMAM) dendrimer amine provides simultaneous electrostatic and covalent interactions between the biomaterial and the tissue, maximizing adhesion. This study finds that the material withstands supra-physiological pressures (≈ 300 mmHg) and prevents bleeding in a rabbit aortic puncture model and in a pig carotid bilateral poly(tetrafluoroethylene) graft model—achieving superior performance to commercially available materials such as Tisseel and BioGlue. Material biocompatibility is validated in comprehensive in vitro and in vivo studies in accordance with the US Food and Drug Administration (FDA) guidelines, including in vitro neutral red uptake test, subcutaneous implantation in rabbits, Ames genotoxicity, and guinea pig maximization test. This material has the potential to provide with adequate seal and reduced complications following complex vascular surgeries, including hard-to-seal tissue-graft interfaces.

pronounced for graft patients (more than half of the patients undergoing surgery) who are treated with antiplatelet therapy for at least one year following surgery.^[3,4] This patient population can greatly benefit from the use of a surgical sealant that serves as a mechanical barrier and reinforces the anastomotic line to prevent bleeding. This has propelled clinical and academic research in this field that resulted in the development of a broad range of adhesive and hemostatic materials that have been approved steadily to treat or prevent bleeding.^[5] Yet, none of the commercially available materials display the properties required to provide with an adequate vascular seal, including: i) lack of biocompatibility or mechanical mismatch between the tissue and the biomaterial—leading to vascular strictures and occlusion, ii) inadequate adhesion under high vascular pressures, and iii) low clinical adoption owing to difficult handling properties. Particularly challenging is the seal of an interface between biological tissues and prosthetic materials, such as in the case of expanded poly(tetrafluoroethylene)

(ePTFE) vascular grafts, because the biomaterial has to bind to very distinct surfaces that require different modes of interaction. The ideal sealant should simultaneously withstand high pressures and display adequate biocompatibility. The material must be flexible and pliable, particularly when sealing small vessels that have a high risk of occlusion. The sealant has to achieve instantaneous crosslinking or display high viscosity to

1. Introduction

Bleeding is one of the most disturbing complication following vascular surgery, with a prevalence of 5%–45%, depending on the type of procedure.^[1,2] This may result from compromised integrity of the anastomotic line or insufficient hemostasis. The risk for late bleeding following surgery becomes even more

G. Muñoz Taboada
BioDevek Inc.
Cambridge, MA 02139, USA


G. Muñoz Taboada
Institut Químic de Sarrià
Universitat Ramon Llull
Barcelona 08017, Spain

P. Dosta, E. R. Edelman, N. Artzi
Institute for Medical Engineering and Science
Massachusetts Institute of Technology
Cambridge, MA 02139, USA
E-mail: nartzi@mit.edu

P. Dosta, N. Artzi
Department of Medicine
Division of Engineering in Medicine
Brigham and Women's Hospital
Harvard Medical School
Boston, MA 02115, USA
E-mail: nartzi@bwh.harvard.edu

E. R. Edelman
Department of Medicine
Cardiovascular Division
Brigham and Women's Hospital
Harvard Medical School
Boston, MA 02115, USA

P. Dosta, N. Artzi
Wyss Institute for Biologically Inspired Engineering
Harvard University
Boston, MA 02115, USA

 The ORCID identification number(s) for the author(s) of this article can be found under <https://doi.org/10.1002/adma.202203087>.

DOI: 10.1002/adma.202203087

properly conform to multiple tissue types and structures. Its delivery should avoid time-consuming and multistep procedures, and ideally eliminate the need for external triggers to initiate crosslinking.^[6]

Commercially available materials rely on the use of low-molecular-weight and highly reactive molecules to create covalent bonds with functional groups on tissue surfaces to afford adhesion. Albumin–glutaraldehyde glues such as BioGlue, achieve their high adhesion strength through the high reactivity of the glutaraldehyde with tissue amines, which impart high intrinsic toxicity.^[7] Cyanoacrylates achieve the required adhesion by the polymerization of its cyanoacrylate monomers in the presence of moisture, which has been associated with a high level of toxicity.^[8] While this approach is able to achieve strong adhesive materials that decrease bleeding complications, many other undesirable adverse events, such as long degradation times or tissue constriction, are often associated with their use.^[9,10] Emerging materials tend to rely on the formation

of noncovalent interactions, alone or in addition to covalent bonds, to enhance adhesion strength. Although weaker, noncovalent interactions such as physical entanglement, hydrogen bonding, and hydrophobic interactions, these bonds synergistically promote adhesion in conjunction with covalent bonds. Noncovalent interactions use chemical groups or tissue traits that differ from those used by chemical bonding, providing complementary binding mechanisms.^[11–15]

Here, we demonstrate that using a sprayable, two-part hydrogel formulation that leverages both covalent and noncovalent interactions we can achieve comparable performance to that displayed by the low-molecular-weight, high-strength materials, such as BioGlue while enhancing material biocompatibility. One part of the hydrogel is composed of generation-5 polyamidoamine (PAMAM)-dendrimer-amine and the other consists of a mixture of oxidized dextran and oxidized alginate whose aldehyde groups form reversible covalent bonds with tissue amines (**Figure 1A**). Oxidized alginate also harbors

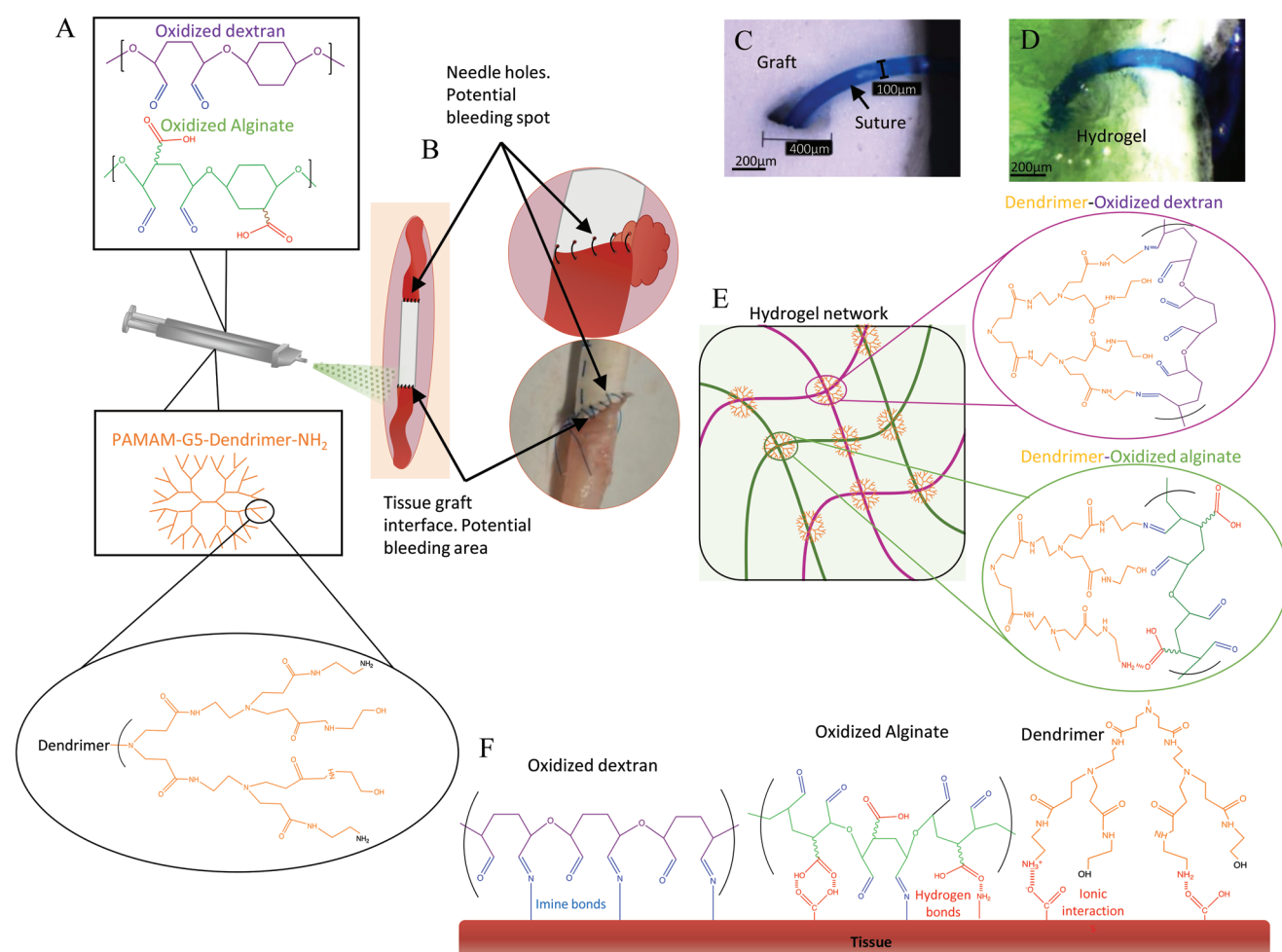


Figure 1. Sealant composition and interactions with tissue and ePTFE graft. A) Scheme of the dual barrel syringe, containing oxidized alginate and oxidized dextran in one chamber, and PAMAM-G5-dendrimer in the second barrel. B) Scheme of the interface between a synthetic vascular graft and the vessel. The anastomotic line as well as the needle-generated holes in the graft are potential bleeding spots that should be sealed. C) Micrography of the ePTFE graft with a single suture point. The size of the needle puncture hole is around 400 μm while the suture diameter is only 100 μm . This mismatch can cause blood leakage through that gap. D) The same suture is depicted following spraying with the Dex:Alg:Den sealant to fully cover the suture line and form a watertight seal to prevent leakage. E) Scheme of the hydrogel network and the interaction between the different components. F) Scheme of the interactions between each of the polymers and biological tissue, covalent interactions in blue and noncovalent in red.

carboxylic acid groups that interact with both the positively charged amine groups in PAMAM dendrimer and with chemical functional groups in the tissue surface such as amines, hydroxyls, and carboxylic acids, providing an additional level of interaction. Excess aldehyde moieties relative to the number of amine groups in the material enable maximizing the interaction with tissue surfaces that display varied density and number of reactive amine groups, yet unreactive aldehyde groups in the material (on dextran and alginate) are consumed internally by the other hydrogel component (dendrimer amine) to afford the formation of the gel while eliminating potential toxicity that is associated with unreacted aldehyde groups. The combination of electrostatic and covalent interactions enables the formation of a strong material that can withstand suprphysiological pressures while maintaining high biocompatibility. The integral covalent and non-covalent interactions afford material adhesion to biological surfaces, while physical entanglement and mechanical interlocking afford interactions with the porous ePTFE graft, securing the tissue:graft anastomotic line. The material was formulated such that it will enable spraying and instantaneous *in situ* crosslinking at the target site to enable clinicians to use it in challenging procedures and in complex geometries (Figure 1B). A comprehensive *in vivo* set of studies was performed, following US Food and Drug Administration (FDA) guidelines for medical devices, and was compared with two predicate materials—Tisseel and BioGlue. We chose Tisseel and BioGlue as they serve as gold standards for biocompatibility and adhesion, respectively. Tisseel, or fibrin glue, is highly biocompatible and has low tissue-adhesion strength, while BioGlue has high adhesion but low biocompatibility and performs similarly to the commercial adhesive Preveleak.^[16] Our goal was to design a material that is as biocompatible as Tisseel, but that also adheres to tissue and graft surfaces to prevent leakage. PAMAM dendrimer:dextran hydrogels have been used preclinically in multiple applications as surgical sealants and as depots for drug or gene therapies due to their high biocompatibility and tunable properties.^[17,18] An optimal material formulation that balances material strength, pliability, and adhesion, while maintaining high biocompatibility is required to achieve adequate tissue:biomaterial interactions that maximize material performance. In this work, we describe how the engineering of a three-component hydrogel, with the addition of alginate to the previously developed dendrimer:dextran hydrogels, enhances both adhesion and cohesion (with tissue and graft surfaces) leading to successful outcomes in vascular procedures in large animal models. We show that dextran:alginate:dendrimer is able to withstand high burst pressures while being pliable to enable adequate sealing of a rabbit aortic puncture and a carotid–graft interface in a pig model.

2. Results

2.1. Material Design and Tissue–Biomaterial Interactions

Our hydrogel is designed to be sprayed over the tissue-graft suture line and adhere to both surfaces. The low viscosity of the polymeric solutions enables the interdigitation and entanglement into the porous graft surface upon spraying, withstanding

high pressures in this complex interface. This procedure has an additional risk of bleeding through the needle hole formed upon suturing the graft to the tissue as the size of the needle is larger than the diameter of the suture itself.^[19] As the graft has no natural hemostatic capacity, bleeding may occur from the suture points (Figure 1C);^[20,19] thus, proper coverage of the suture can provide an extra degree of sealing to the anastomotic line (Figure 1D).

Both polysaccharides can interact internally with the dendrimer through aldehyde–amine interactions (Figure 1E) and externally with the tissue (Figure 1F). Using IR spectroscopy, we confirmed the presence of aldehyde carboxyl (C=O) bonds, validating the oxidation of both dextran (Figure S1A, Supporting Information) and alginate (Figure S1B, Supporting Information). The aldehyde groups provided a small peak (1732 cm⁻¹) due to the formation of intramolecular hemiacetal groups, which are widely described in the aldehyde-containing polymers when in the dry state.^[21–23] The presence of the aldehyde groups was also confirmed using H-NMR (Figure S2, Supporting Information).

2.2. Optimizing Adhesive Hydrogel Sprayability and Performance

We studied the effect of oxidized dextran, oxidized alginate, and dendrimer on hydrogel properties such as gelation time, swelling, and compressive strength. Gelation time has to be optimized for *in vivo* use to enable rapid crosslinking following application such that the sealant will remain in place. The gelation time should be long enough to not clog the applicator, to provide time for material interdigitation and mechanical interlocking with the tissue, as well as to adhere to the tissue surface it is sprayed onto without flowing. We tested different dextran/alginate ratios with a total solid concentration of 15%w/w in the polysaccharide part of the sealant at three dendrimer concentrations of 10% (Figure 2A), 15% (Figure 2B), and 30% (Figure 2C). We obtained gelation times ranging from 5 to 150 s, which provides flexibility in using this family of materials for diverse applications. We found that oxidized dextran and dendrimer are the two components with a greater impact on the gelation time. We then studied the swelling behavior for the same dextran/alginate ratios at 10% (Figure 2D), 15% (Figure 2E), and 30% (Figure 2F) dendrimer concentrations. While the increase in the concentration of oxidized dextran and dendrimer increases the crosslinking density and therefore decreases swelling, oxidized alginate which contains hydrophilic carboxylic acid groups increases the water absorption. Also, some formulations with high alginate content resulted in hydrogels with high hydrophilicity that leads to continuous swelling causing their rapid degradation within 24 h (Figure S3, Supporting Information). To better understand the hydrogel stability and the role of each component in forming the network structure we also studied the water content of these formulations over time (Figure S4A–C, Supporting Information). Those formulations with higher alginate content, displayed sustained water uptake into the network reaching values of 95% water content. We quantified material gel fraction (Figure S4D–F, Supporting Information) to understand the swelling and water

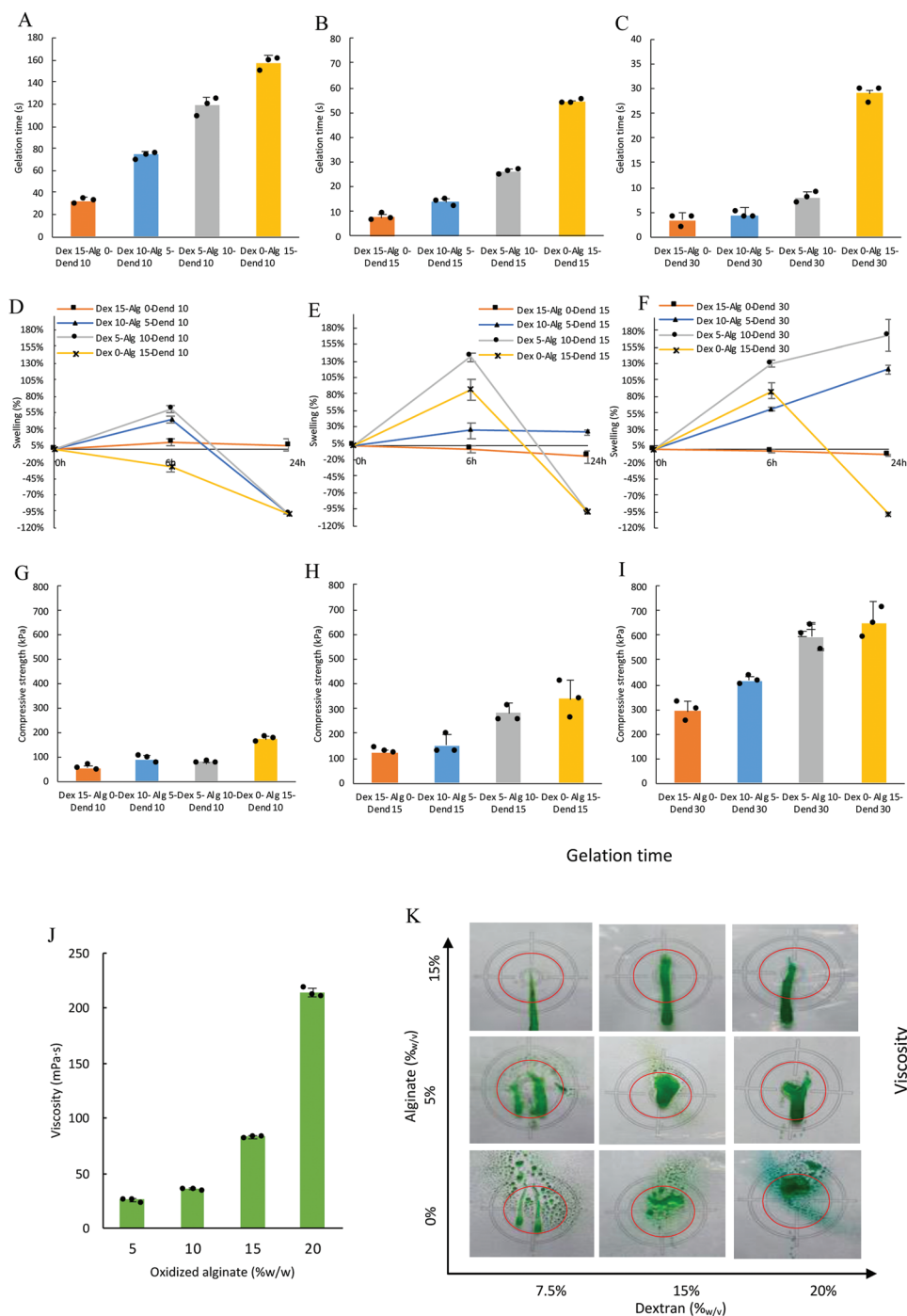


Figure 2. Formulation impact on hydrogel properties and spray pattern. Gelation time is influenced by the concentration of each component. A–C) Different ratios between the polysaccharides were tested, combined with 10% (A), 15% (B), and 30% (C) dendrimer concentrations ($n = 3$). D–F) Swelling of the hydrogels at 0, 6, and 24 h at 37 °C shows a strong impact on hydrogel stability for different dextran/alginate ratios at 10% (D), 15% (E), and 30% (F) dendrimer concentrations ($n = 3$). G–I) Effect of dextran/alginate ratio on the compressive strength at 10% (G), 15% (H), and 30% (I) dendrimer concentrations ($n = 3$). J) Viscosity of 15% oxidized dextran with different concentrations of oxidized alginate. Data are presented as mean \pm standard deviation (SD), $n = 3$. K) spray pattern of 30% dendrimer formulations combined with different concentrations of oxidized dextran and oxidized alginate. The oxidized polysaccharides promote adequate airless spray pattern. Increasing alginate concentrations increases the viscosity, creating a less dispersed spray pattern. Increasing dextran concentration significantly reduces gelation time, minimizing the dripping when sprayed onto a vertical surface.

content behavior of the hydrogels. While some of the formulations seem to swell significantly, that is often accompanied by a decrease in gel fraction of the material, thus contributing

to rapid hydrogel degradation. We then studied the role of the three polymeric components in determining the compressive strength of the material. We tested a range of dextran/alginate

ratios, at dendrimer concentrations of 10% (Figure 2G), 15% (Figure 2H), and 30% (Figure 2I). Dendrimer and alginate solid content considerably affect material compressive strength compared to the dextran owing to the internal ionic interactions between the alginate carboxylic acids and dendrimer amines as well as their interactions with the tissue.

To study the sprayability of our material we used an airless device applicator commercialized by Ethicon for their fibrin products. The adaptor connects two syringes to the spray nozzle. We found that the viscosity of the polysaccharide mixture is dictated by the oxidized alginate concentration (Figure 2J). We then studied the effect of oxidized alginate (driver of viscosity) and oxidized dextran (driver of gelation time) concentrations on the spray pattern (Figure 2K) by spraying 2 mL of sealant using an airless device onto a 10 cm in diameter vertical target. The increase in oxidized alginate solid content increased the viscosity of the mixture, creating a less spread, stream-like pattern. The increase in dextran solid content did not increase the viscosity of the mixture; however, it had a strong impact on gelation time—making it gel faster, minimizing the dripping of the sprayed material on the vertically positioned target. To confirm the stability of the oxidized polysaccharides after lyophilization, we tested the gelation time of two different formulations of different batches of oxidized dextran and oxidized alginate that had been stored for less than ≈ 1 month, ≈ 6 months, and ≈ 1 year at 4 °C in a lyophilized state. There were no changes in the gelation time, which indicates that the polymers did not undergo significant degradation (Figure S5, Supporting Information).

2.3. Burst Pressure Optimization in Ex Vivo Models

We then studied the role of each component on the burst pressure—the highest pressure that a material is able to withstand prior to bursting. We have adapted the ex vivo ASTM method^[24] to our specific application using freshly harvested pig small intestine. We created a 3 mm hole in the middle of the tissue and added a loose suture to bring the edges of the hole together (Figure 3A). Before each test, we confirmed, by a preburst test, that the suture was not able to hold any pressure.

We first tested the effect of the dendrimer solid content, when mixed with oxidized dextran on the burst pressure. This formulation, 10% Dex–15%Den, matches our previous adhesive formulation that has been used in other applications, as reported by us^[17] achieving burst pressure values in the range of 30–40 mmHg in this model. By increasing the dendrimer content from 10% to 30% we observed a sixfold increase in the burst pressure, achieving values of 130 mmHg (Figure 3B). We hypothesized that the increase in burst pressure associated with the increase in the content of PAMAM dendrimer is due to the increased crosslinking density of the material, which enhances its cohesion strength, as well as the interaction with the tissue due to hydrogen bonds and electrostatic interactions between the positively charged amine groups on the dendrimer with negatively charged groups on the surface of the tissue, such as carboxylic acid.

The addition of the oxidized alginate to the mixture enhanced the burst pressure to suprphysiological values, above 200 mmHg (Figure 3C). The higher the alginate content,

the higher the burst pressure was. However, its solid content is limited by its sprayability owing to the increase in viscosity produced by its larger molecular weight compared to the 10 kDa dextran. Oxidized dextran has not had a strong impact on the burst pressure achieved in this model, hence a concentration of at least 10% dextran was fixed to provide adequate hydrogel stability that is otherwise compromised below that solid content (Figure 3D). The hydrogel comprising 15% dextran, 10% alginate, and 30% dendrimer, displayed the highest burst pressure with levels of 263 ± 38 mmHg in the ASTM model. We postulate that the increase in dextran solid content, that is, the increase in the number of available reactive aldehyde groups, has not imparted a notable increase in burst pressure due to the saturation of the available tissue amines to react with the aldehyde groups in the sealant.

While the ASTM test method is ideal for material optimization studies, we tested a selection of the higher-performing material formulations in an ex vivo model that recapitulates the in vivo scenario, using an ex vivo end-to-end anastomosis model between pig carotid and the ePTFE graft (Figure 3E). The material needs to provide proper adhesion to the biological tissue and to the synthetic material, and seal the ≈ 30 suture needle punctures created to afford a tight seal. We used BioGlue, comprised of 10% glutaraldehyde and 45% bovine serum albumin, as a control representing a material with high burst pressure and Tisseel, a commercial brand for fibrin glue, as a material that displays relatively low adhesion strength that is not anticipated to suffice in this challenging application.

Similar to the ASTM model, before each test we performed a pre-burst run to confirm that the suturing alone was not able to hold more than 10–15 mmHg. In this model, we measured the adhesion capacity and the ability of the material to prevent leakage when applied circumferentially onto a vessel-graft construct. Some of the formulations (with higher total solid contents) displayed slightly compromised performance due to the excessively fast crosslinking and the lack of sufficient time for forming interactions with the substrate. The formulation containing 15% dextran, 5% alginate, and 30% dendrimer provided the best overall performance with a burst pressure of 300 ± 38 mmHg, comparable to that of BioGlue. Beyond ≈ 300 mmHg, the clinically used ePTFE graft, a highly porous material, started leaking through the porous matrix, as it is not designed to hold such high blood pressure. Tisseel, which is known to provide limited adhesion, displayed a value of 50 mmHg (Figure 3F). Further mechanical characterization of 15Dex:10%Alg:30%Den and 15Dex:5%Alg:30%Den can be found in Figure S6 (Supporting Information).

2.4. Sterilization Using Gamma Irradiation

Toward scale-up manufacturing, industrial methods for material sterilization, such as radiation, are used in place of the bench-top 0.2 μm filtration. Many polymers are not compatible with radiation as their structure can be damaged and mechanical or chemical properties modified. To confirm that large-scale sterilization techniques would not affect the performance of our material we tested a high dose of 20 kGy and then

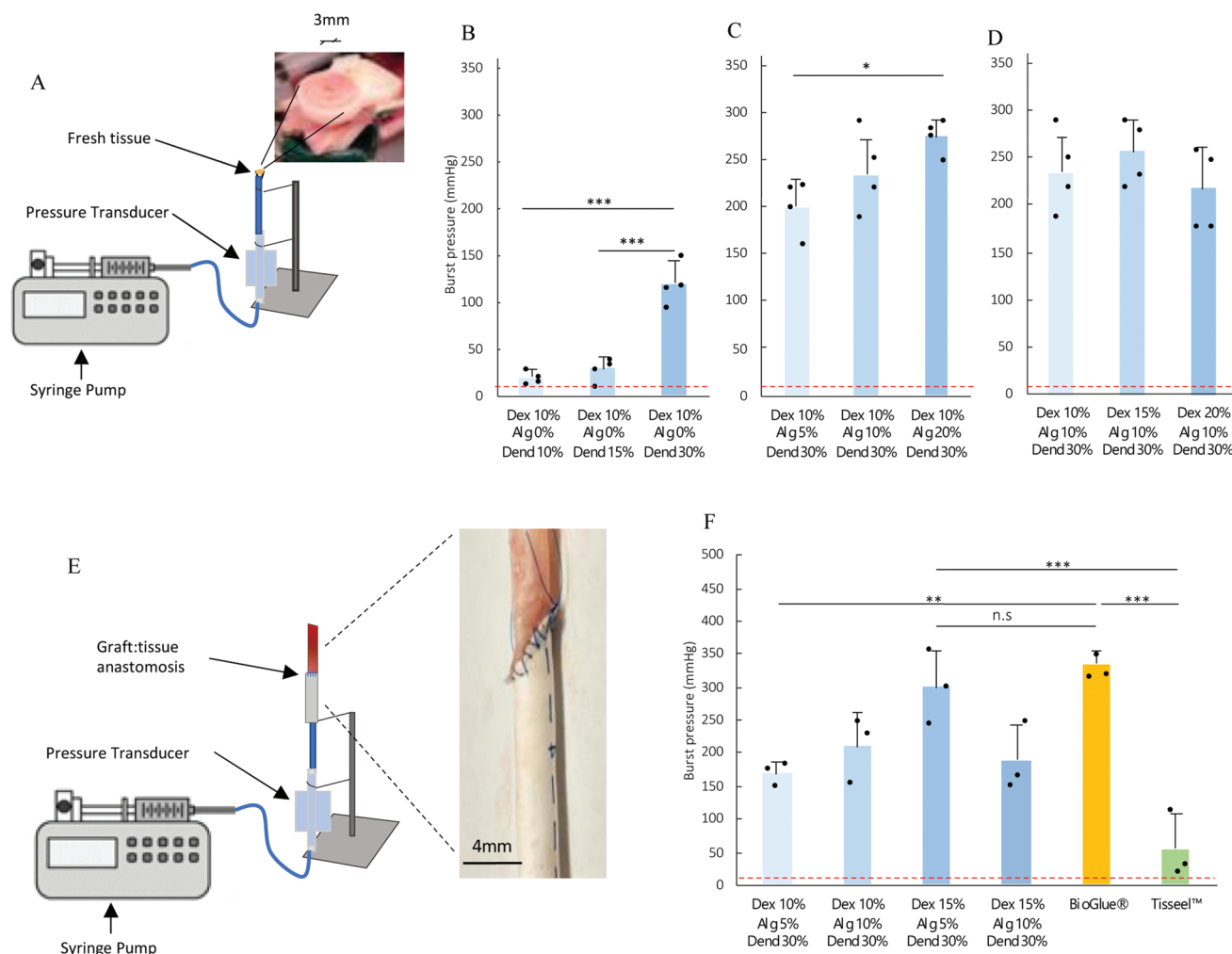


Figure 3. Burst pressure ex vivo gastrointestinal and carotid models. A) A scheme showing the burst pressure setup used to optimize the sealant formulation. B–D) Burst pressure data as a function of: B) PAMAM dendrimer solid content of C) oxidized alginate and D) oxidized dextran. Data are presented as mean \pm SD, $n = 4$. The red line represents the baseline burst pressure that a single suture can withstand, 10–15 mmHg. E) In vitro burst pressure of the graft:tissue anastomosis. F) Burst pressure values of the Dex:Alg:Den sealant in the in vitro graft:tissue anastomosis model compared to controls. The red line represents the pressure that the sutures alone were able to withstand. Data are presented as mean \pm SD, $n = 3$. P -values were calculated using a two-sided t -test. * $P < 0.05$, ** $P \leq 0.01$, *** $P \leq 0.001$.

40 kGy. We confirmed that the gelation time was not affected by the sterilization under the tested conditions. Quantifying small changes in the gelation time of the actual formulation is challenging because the material is designed to gel within seconds. To maximize potential variations in gelation times, the formulation 15%Dex:5%Alg:30%Den was diluted in three, slowing the gelation time to about 40s. Now, differences in gelation time for different formulations are detectable, yet, no differences were found as a result of radiation (Figure 4A). The burst pressure of our sealant was not modified by gamma irradiation at a dose of 20 kGy—a standard dose for sterilization of medical devices. A very high dose of 40 kGy decreased the burst pressure in about 50% (Figure 4B). To understand if the gamma irradiation has any effect on the degradation profile of the bulk material, we tracked the material degradation over 30 d. No significant differences were found before and after irradiation (Figure 4C).

2.5. In Vitro Biocompatibility

Adhesive materials contain polymers that interact with tissue proteins and cell surface molecules by design, which is expected to induce some levels of cytotoxicity. We performed a comprehensive study of the biocompatibility of both the sealant and its individual components. The imine chemistry that forms the hydrogel creates a reversible bond that hydrolytically degrades over time without the need for enzymatic degradation, releasing the initial polymeric components rather than degrading them into the basic monomeric units. We performed neutral red uptake (NRU) assay—an FDA-recommended test for evaluating the cytotoxicity of medical devices^[25] (see Figure S7, Supporting Information, for details). The NRU assay consists of treating L929 mouse fibroblast for 24 h with the material to be studied. When testing the individual components, we dissolved them into Dulbecco's modified Eagle's medium (DMEM) media and

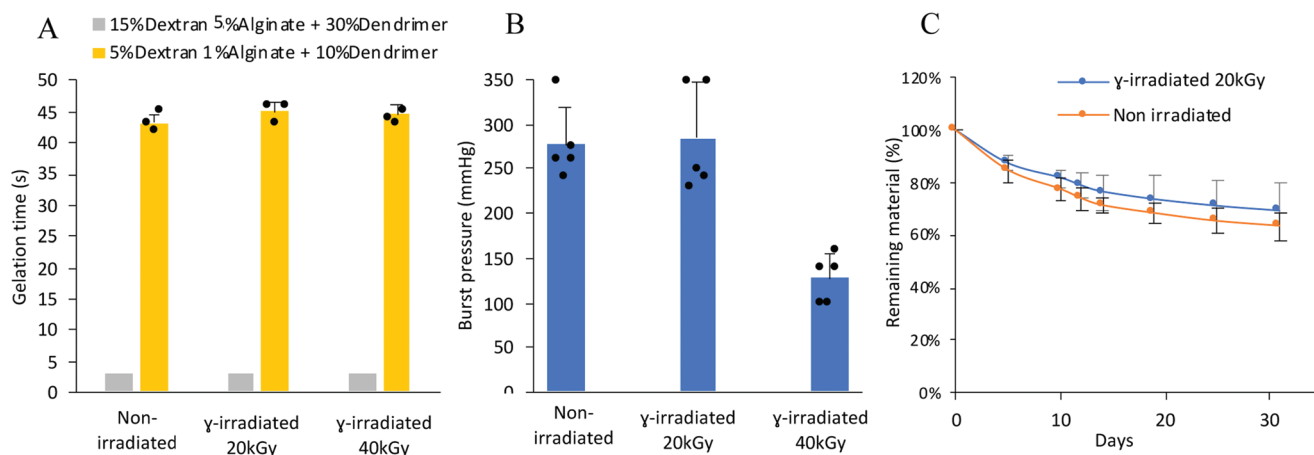


Figure 4. Impact of gamma sterilization on hydrogel properties. Effect of gamma irradiation on A) gelation time using the selected formulation and its 3:1 dilution to slow down the crosslinking and enable accurate measurements as a function of radiation dose ($n = 3$). B) Burst pressure using a 3 mm puncture model in small intestinal tissue of the 15% Dex:5%Alg:30%Den formulation ($n = 5$), and C) in vitro degradation, before and after 20 kGy gamma irradiation ($n = 9$). Data presented as mean \pm SD.

were directly applied to the cells. When testing gelled sealant, we incubated the hydrogels for 24 h at 37 °C in DMEM media that was then applied to the cells for a period of 24 h before measuring the cytotoxicity. The individual polymer components do not present any toxicity when tested using 0.05–5 mg mL⁻¹. Although the oxidized alginate and dextran contain aldehyde groups within their chains, their high molecular weight minimizes cytotoxic effects. While PAMAM dendrimers may induce cytotoxic effects due to their strong cationic nature, 75% of the amine groups on the surface of the PAMAM dendrimer have been modified with hydroxyl groups in our formulation, leading to high cell viability 90 \pm 5% even at a concentration of 5 mg mL⁻¹ (Figure 5A). Alginate, having a higher molecular weight than dextran, had cell viability of 89 \pm 2% at 5 mg mL⁻¹ (Figure 5B), while 10 kDa dextran imparted a decrease in cell viability (68 \pm 4%) only at the highest dose of 5 mg mL⁻¹, which is well above its physiological concentration as the material slowly degrades over time (Figure 5C).

To properly assess the cytotoxicity level of our formulations, we used BioGlue as a positive control (representing high cytotoxicity) and Tisseel as a negative control (representing low cytotoxicity) (Figure 5D). This assay entails exposing the cells to the material extract for 24 h and then assessing the cell viability. Several of our top performing formulations, with oxidized dextran content ranging from 10% to 15%, alginate from 5% to 10%, and dendrimer at 30%, displayed cell viability values greater than 90%, matching the Tisseel results. BioGlue, a commercially available material achieves only 30% cell viability. We confirmed that the gamma irradiation sterilization process did not affect significantly the cell viability results of the individual components (Figure S8, Supporting Information).

We tested the hemocompatibility of the material, as it may come in contact with blood during its application, for oxidized dextran, oxidized alginate, and dendrimer at concentrations ranging from 1 to 50 mg of polymer per mL of blood. We also tested the final hydrogel at 20–200 mg of hydrogel per mL of blood. These concentrations are suprphysiological and enable studying the blood reactivity at a broad range of concentrations.

All the hydrogel concentrations displayed neglectable hemolysis, under 0.2% (Figure S9, Supporting Information), which is 30-fold below the recommended 5% limit.^[26,27]

2.6. Rabbit Subcutaneous Implantation

Next, we evaluated the biocompatibility of our sealant in vivo in a rabbit subcutaneous implantation model at days 7, 14, and 30. We compared four different Dex:Alg:Den formulations using Tisseel and BioGlue as controls. We surgically implanted six samples in each rabbit, that were well separated to allow the pathologist to study the responses to individual material (Figure 5E) (a detailed layout and position of the implants is displayed in Figure S10A,B, Supporting Information). Each of the different families of implanted materials—15%Dex:5%Alg:30%Den adhesive hydrogel (Figure 5F), BioGlue (Figure 5G), and Tisseel—displayed different morphology at day 30 (Figure 5H). We studied the biological responses to the materials in the local tissue:material interface over time to validate that there are no unexpected adverse outcomes (Figure S11A–F, Supporting Information) according to the scoring system displayed in Figure S11G (Supporting Information). Based on histology images from the three material families, BioGlue maintains its stiff and solid nature after 30 d (Figure 5G) while Tisseel exhibits a fibrous structure which is attributed to its fibrinogen and thrombin composition (Figure 5H). 15%Dex:5%Alg:30%Den sealant displays more advanced degradation after 30 d, while maintaining an intimate contact with the surrounding tissue (Figure 5F). The degradation of the material over the course of a few weeks may enable better tissue regeneration and restoration of tissue properties, while maintaining tissue adhesion to avoid delayed leakage. While fibrosis (Figure 5I) and neovascularization (Figure 5J) seem to stabilize in the Dex:Alg:Den group by day 14, it continued increasing in the BioGlue and the Tisseel groups through day 30. Our sealant displayed lower degenerative-necrotic exudate levels that were not seen in the other groups,

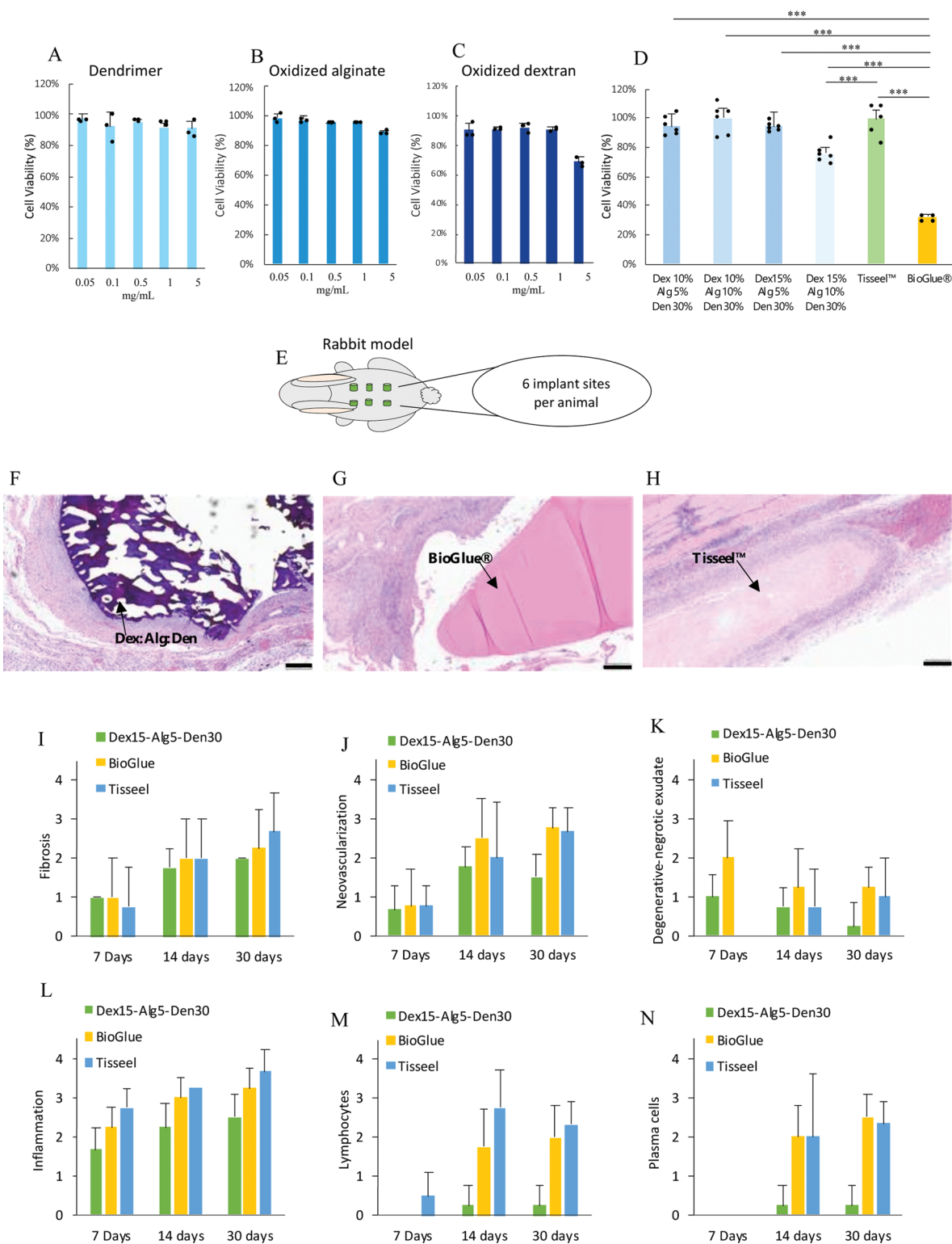


Figure 5. In vitro cell viability and 30 d in vivo subcutaneous implantation biocompatibility studies of 15%Dex:5%Alg:30%Den, BioGlue, and Tisseel. A–C) Neutral red uptake test for the individual components of the sealant dendrimer (A), oxidized alginate (B), and oxidized dextran (C) ($n = 3$). D) Neutral red uptake test of the optimized sealant formulations performed with the material extract using a ratio of 0.2 g of material per mL of extraction media ($n = 6$). E) Scheme of the rabbit implant location. F–H) Representative images of H&E staining at day 30 of 15%Dex:5%Alg:30%Den (F), BioGlue (G), and Tisseel (H); scale bar = 200 μm . I–N) Macroscopic observations and cell infiltration of fibrosis (I), neovascularization (J), degenerative necrotic exudate (K), inflammation (L), lymphocytes (M), and plasma cells (N) at the rabbit subcutaneous implantation sites ($n = 4$) at 7, 14, and 30 d. Data presented as mean \pm SD. P -values are calculated using a two-sided t -test. * $P < 0.05$, ** $P \leq 0.01$, *** $P \leq 0.001$.

although Tisseel is considered the gold-standard material in biocompatibility studies (Figure 5K). Based on the cellular infiltration into the implant sites, the inflammation in both BioGlue and Tisseel groups was moderate, which most likely stems from the implantation procedure itself and the presence of foreign material. Dex:Alg:Den sealant displayed a slightly lower inflammatory response compared to the two commercially available materials but still within the same range (Figure 5L). Both BioGlue and Tisseel contain animal- or human-derived materials, respectively, which have the potential to trigger a more immunogenic response, as seen by the high level of lymphocytes (Figure 5M) and plasma cells (Figure 5N) throughout the study. This study confirmed that our material displays a biological response in vivo that is comparable to that of the FDA approved materials. Representative images for the H&E and Masson's trichrome (MTC) staining at day 30 are depicted in Figure S12 (Supporting Information) for all the materials, and their magnified insets are depicted in Figure S13 (Supporting Information).

2.7. Guinea Pig Sensitization

The potential of allergic reaction caused by the material may not be captured by subcutaneous implantation studies due to the single application and small population. To assess the material allergenic potential in a large population, Guinea Pig Kligman sensitization assay, an FDA-required assay, was performed. This assay uses extracts of the tested material. The extracts are injected intradermally at day 0, topically (wet sponge) at day 7 for 48 h, and again topically at day 23 for 24 h to the same spot, favoring the generation of an allergic response. Potential allergic reactions are recorded at day 24, 25,

and 26. 15%Dex:5%Alg:30%Den formulation was extracted in a polar (saline) and nonpolar (cotton seed oil) media at 50 °C for 72 h. A group of 20 animals were intradermally injected with the material extract (10 polar, 10 nonpolar) at day 0. Dinitrochlorobenzene ($n = 5$) and saline ($n = 10$) were used as positive and negative control, respectively. At day 7 the material extracts were applied topically (within a patch) for 48 h at the intradermal injection sites. The 24 h challenge phase was then performed on day 23 with another topical application. The animals were scored for erythema and edema according with the Magnusson and Kligman Scale at 24 h, 48 h, and 72 h post challenge (Figure 6A). In the animals tested with Dex:Alg:Den extracts, no visible change was observed (Figure 6B) in any of the animals tested (Figure 6C). This result confirmed that Dex:Alg:Den materials do not cause sensitization.

2.8. Ames Genotoxicity Assay

To further minimize potential safety concerns along the translational process, genotoxic or mutagenic effects caused by the material should be ruled out. We performed the *Salmonella typhimurium* reverse mutation assay (Ames test), which is a short-term bacterial test for the identification of carcinogens using mutagenicity in bacteria as an endpoint (Figure 7A). The test material is first extracted in polar (saline) or nonpolar (DMSO) solvents for 72 h at 70 °C (Figure 7B). The extraction media is then applied on top of an agar plate of different bacterial strains that are unable to grow without the supplementation of histidine or tryptophan. After 72 h of incubation in the absence of histidine and tryptophan, the bacterial colonies are counted. The number of colonies found is directly related with the ability of the tested material to cause mutations and

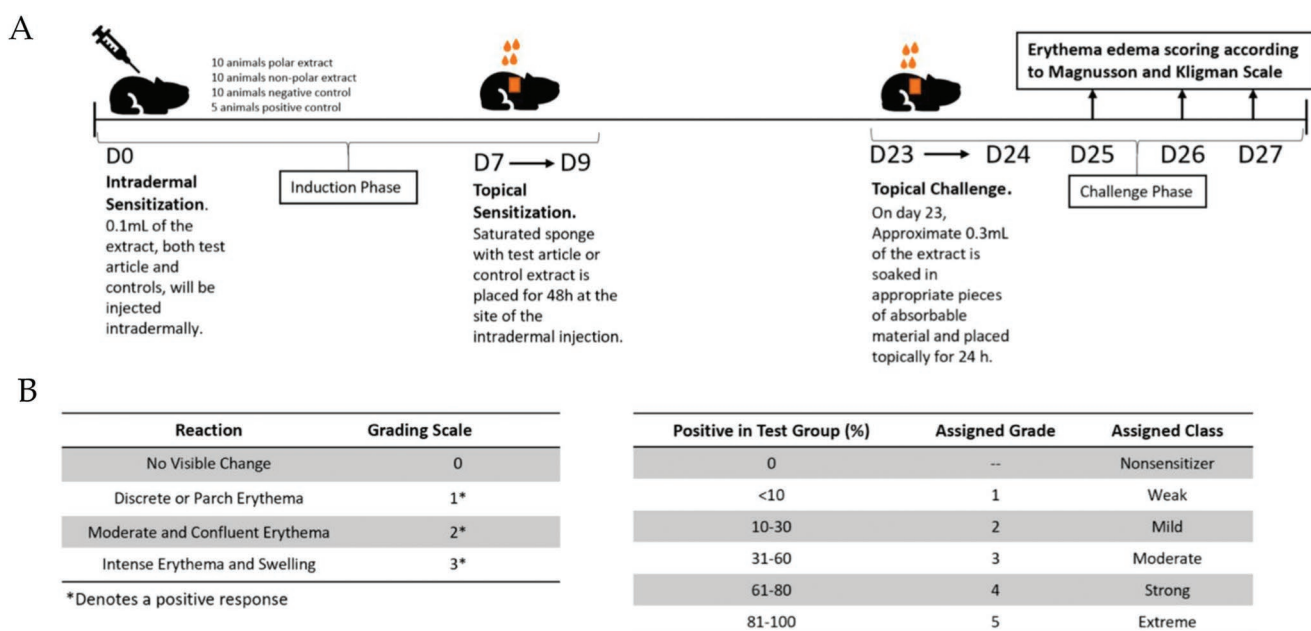


Figure 6. Guinea pig Kligman sensitization study. A) Guinea pigs are injected with the material extract on day 1, on day 7 the extract is placed at the site of injection for 48 h. On day 23 the animals are challenged again with an extract application. B,C) The degree of reaction (B), as well as the number of animals showing any reaction (C) is recorded. Positive control $n = 5$, negative control $n = 10$, Dex:Alg:Den group $n = 20$.

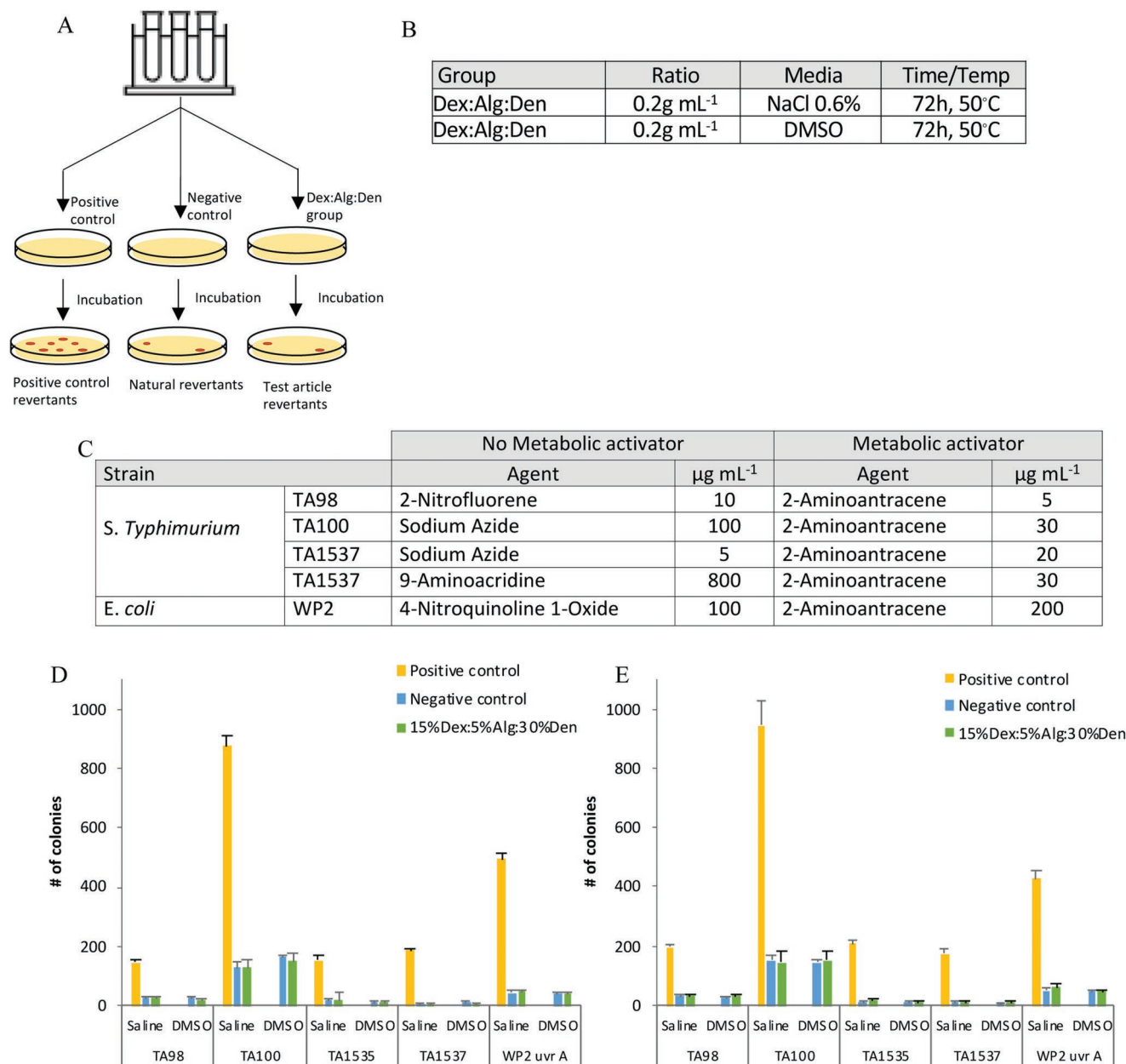


Figure 7. Genotoxicity reverse mutation Ames assay. A) 15%Dex:5%Alg:30%Den extracts, positive (mutagenic) and negative (nonmutagenic) controls are administered on top of agar plates with bacterial strains unable to grow without histidine (*S. typhimurium*) or tryptophan (*E. coli*). B) Dex:Alg:Den materials are extracted using two different solvents to capture polar and nonpolar leachables. C) The potential mutagenic effect of the Dex:Alg:Den material is tested against five different bacterial strains, each one of them with specific known mutagenic as positive control. D) The number of colonies without the addition of metabolic activators is quantified for the three groups, both polar and nonpolar media in the five different bacterial strains. E) The number of colonies with the addition of metabolic activators is quantified for the three groups, both polar and nonpolar media in the five different bacterial strains. Data presented as mean \pm SD, $n = 3$.

thereof reverse the mutation of the deletion of the histidine or tryptophan. Each bacterial strain has its own positive control (Figure 7C) and every extract is tested under two conditions, without (Figure 7D) or with (Figure 7E) metabolic activator which is a pro-mutagen activator. In Figure 8D,E, we show one of the four different Dex:Alg:Den tested. All the formulations tested provided nonmutagenic results (Figure S14, Supporting Information). Testing multiple formulations of the Dex:Alg:Den platform enabled us to confirm that the non-genotoxicity is

associated with the material platform rather than a single formulation.

2.9. Rabbit Aorta Puncture Sealing

We next evaluated the ability of the Dex:Alg:Den sealant, and the control materials, to achieve instantaneous hemostasis and to withstand blood pressure over a period of 5 d following aortic

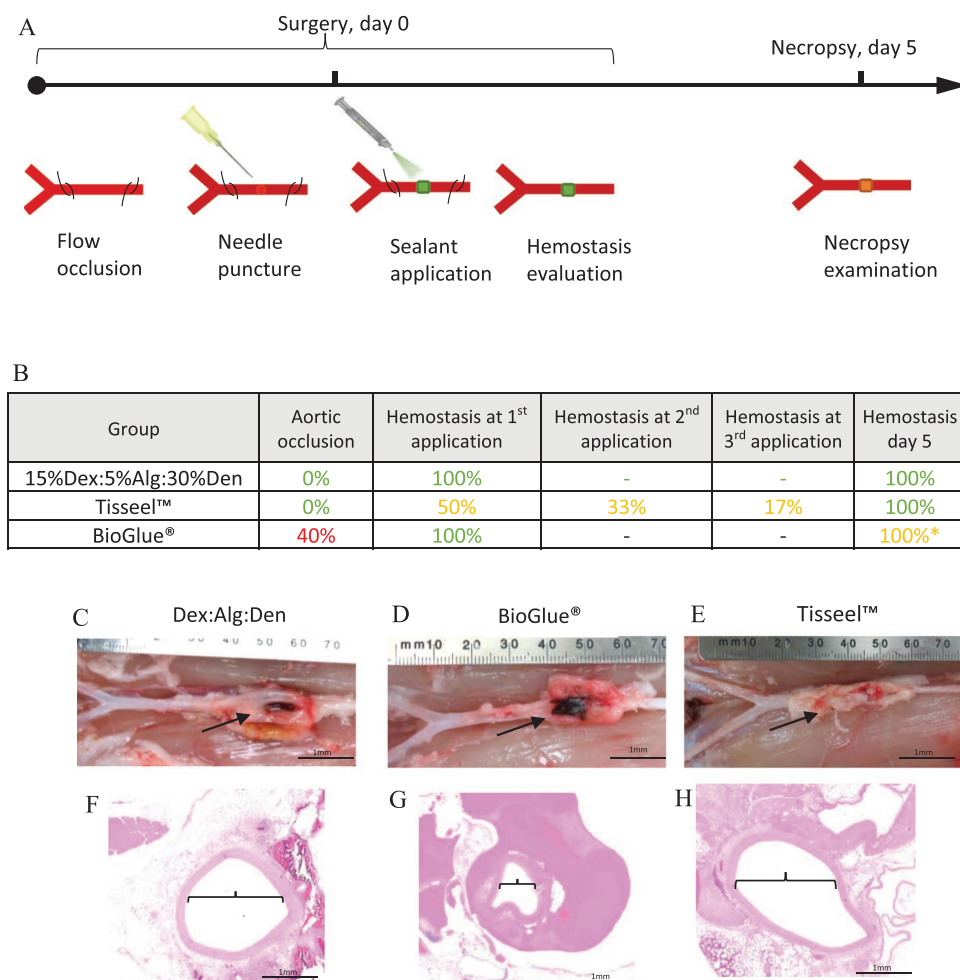


Figure 8. Rabbit aortic puncture model achieving hemostasis at 0 and 5 d. A) Timeline of the in vivo study and the key steps during the procedure and necropsy. B) Material performance in vivo. C–E) Aorta puncture site for 15%Dex:5%Alg:30%Den (C), BioGlue (D), and Tisseel (E) in a rabbit model at day 5. F–H) H&E slides depict the vessel diameter for 30%Dex:5%Alg:15%Den (F), BioGlue (G), and Tisseel (H); scale bar = 1 mm. $n = 6$ for 15%Dex:5%Alg:30%Den and Tisseel, $n = 5$ BioGlue. *Two out of five animals from the BioGlue group had to be euthanized due to aortic occlusion but the other three displayed appropriate hemostasis at day 5.

puncture (using 21-G needle to form a 1 mm puncture in the aorta of about 2–3 mm in diameter) while allowing the vessel to heal. The aorta was isolated, and the aortic puncture was performed below the renal arteries to guarantee blood supply to the abdominal organs via blunt dissection. Proximal and distal regions of the aorta were occluded using umbilical tape following heparin (1000U, IV) administration. Bleeding at the puncture site was visually confirmed and then treated with our adhesive or the control materials (Figure 8A).

Using a spray applicator, a thin layer of Dex:Alg:Den sealant was applied to cover the full aorta circumference. Dex:Alg:Den sealant was designed to provide immediate gelation to ensure that the material will remain on site and will not flow or drip. This allows for an accurate and convenient application in a range of locations and geometries. All Dex:Alg:Den treated animals were able to achieve and maintain hemostasis at time 0 till necropsy time. Half of the Tisseel-treated animals required multiple applications to achieve hemostasis at t0. In the BioGlue group, two animals had to be euthanized due to excessive narrowing of the aorta, which led to bilateral

hindlimb paralysis on day 1. Hindlimb paralysis was attributed to compromised blood flow to the caudal extremities caused by BioGlue-related stenosis (Figure 8B). Dex:Alg:Den sealant (Figure 8C) displayed golden-dark color associated with the formation of the imine bond upon crosslinking. BioGlue which shares the same chemistry exhibits similar color (Figure 8D), while Fibrin glue which undergoes enzymatic crosslinking presents with a white, fibrous appearance (Figure 8E). In the histological analysis, both 15%Dex:5%Alg:30%Den (Figure 8F) and Tisseel (Figure 8H) maintain an open lumen while the BioGlue (Figure 8G) caused severe narrowing of the aorta, which is aligned with the morbidity seen in its group.

2.10. Carotid End-to-Side Vascular Graft Anastomosis in a Pig Model

We next sought to demonstrate the efficacy of Dex:Alg:Den sealant in a more challenging and clinically relevant model. We chose a pig bilateral carotid end-to-side vascular graft

anastomosis—a model in which the sealant must provide hemostasis around the suture line at the interface of the tissue and the ePTFE graft, in a highly heparinized animal. During the procedure, both carotids undergo a graft placement, with an initial vessel diameter of 4–6 mm. While in a clinical surgical procedure the surgeon confirms that there is no immediate leak following suture placement in order to provide with a tight anastomotic line, we sought to test material performance under more challenging conditions. Hence, we applied the material while some oozing from the suture line was still evident. In addition, aspirin and clopidogrel were administered daily following the surgery serving as anticoagulant and antiplatelet therapies, respectively, similarly to the treatment regimen used in high-risk patients. Anticoagulant and antiaggregant therapies are able to maintain a high risk of bleeding through the study period. The placement of the ePTFE grafts entails a microsurgery that requires highly skilled surgeons. The suturing of one graft only can last up to 1 h, during which the blood flow is occluded. This results in arterial vasospasm, leading to considerable narrowing or constriction of the vessel. At that point the material is being applied, prior to restoring blood flow (Figure 9A). The biocompatibility of the material and its mechanical compliance are critical in enabling the vessel to restore itself and expand to its initial size. This represents a challenge in material design, as the material must be strong enough to withstand the high blood pressure, while being flexible to enable vessel recovery. An Angiography was performed to measure the initial vessel diameter of each animal for Tisseel (Figure 9B-I), BioGlue (Figure 9C-I), and 15%Dex:5%Alg:30%Den (Figure 9D-I) groups. We also recorded the diameter of the vessel at the suture lines, right after sealant application for Tisseel (Figure 9B-II), BioGlue (Figure 9C-II), and 15%Dex:5%Alg:30%Den (Figure 9D-II), and the diameter on day 14, prior to necropsy for Tisseel (Figure 9B-III), BioGlue (Figure 9C-III), and 15%Dex:5%Alg:30%Den (Figure 9D-III) to evaluate vessel recovery.

One of the animals in the Tisseel group had to undergo an emergency surgery a few hours after the procedure because of a growing hematoma in the neck which ≈600 mL of blood to be removed. The bleeding source could not be determined but could be due to improper sealing by Tisseel of one of the suture lines. We also found that one of the carotids treated with BioGlue was completely occluded at the time of pre-necropsy angiography (Figure S15, Supporting Information). This result corroborates the data obtained in the rabbit aorta model. In the rabbit model, the vessel treated with BioGlue that was occluded, was relatively small (2–3 mm), while in this study the swine carotid had a much larger diameter of 5–6 mm. This points at a potential vessel occlusion not only in small vessels but also in medium-to-large ones. We performed quantitative vascular analysis to study vessel recovery following each of the four treatments per animal (two suture lines per graft, two carotids per animal) by measuring the diameter after sealant administration (t_0) and prior to necropsy at day 14. Vessel recovery in the Dex:Alg:Den group was comparable to that seen in the Tisseel group, while no recovery was observed in the BioGlue group (Figure 9E). Histological analysis of the tissue-graft interface displayed that 15%Dex:5%Alg:30%Den (Figure 9F) and Tisseel (Figure 9G) resulted in less pronounced neointima

layer formation than BioGlue group (Figure 9H). The combination of the limited diameter recovery and the neointima hyperplasia was likely the cause of the occlusion of one of the animal carotids. The 15%Dex:5%Alg:30%Den material represents the only sealant that provided an adequate seal while enabling vessel recovery.

3. Discussion

The development of new emerging sealant technologies requires the identification and exploitation of new mechanisms of tissue–biomaterial interactions to achieve improved adhesion while maintaining high biocompatibility. There is a wide range of strategies that have been used to achieve that, including mimicking natural adhesion mechanisms,^[28] using external triggers to enhance material properties,^[29] or using precast materials.^[14] Many of these materials gel or adhere to tissue following external triggers including light application or oxidative components^[13,29,30] that can compromise the safety profile of the material as well as create a multistep protocol that may limit their clinical adoption. Precast materials, such as in a bandage form, have been implemented leveraging non-covalent interactions.^[15] However, the bandage delivery strategy may limit the application to certain geometries where a sprayable material has the potential to achieve complete coverage. Also, to achieve full strength, some of these technologies would require clinicians to apply pressure for what may be considered an excessive amount of time (up to 30 min) during surgery.^[14] Here, we combined a well-characterized dextran-dendrimer hydrogel with alginic acid to afford the combination of covalent and noncovalent interactions.

Dex:Alg:Den sealant was designed to maintain low viscosity to enable its sprayability, while the multivalent dendrimer provided with an instant crosslinking. The use of imine chemistry provides fast crosslinking and suture line coverage without flowing or leaking following application in the absence of external stimuli such as UV-light or other multistep approaches.^[31,32] Also, we show that the use of reversible imine chemistry, enables biodegradation of the material without the need of enzymes or external triggers. Since the use of materials that combine multiple adhesion mechanisms has been proven to be a promising approach to achieve strong adhesion to biological and non-biological substrates,^[33] we leveraged the negatively charged alginic acid to provide carboxylic groups that can interact with multiple moieties in the substrate providing an enhanced degree of adhesion.^[11,34,35] Our preclinical work corroborates published mechanistic and computational models demonstrating the potential of multimechanism-mediated adhesion in overcoming the challenges of existing materials. We corroborated that the use of different adhesion mechanisms (ionic and covalent) can provide a synergy in terms of adhesion strength, as well as limiting the toxicity that would be otherwise needed to achieve those adhesion values. We have demonstrated that covalent and noncovalent internal and external interactions can be successfully applied to (pre)clinical procedures. By tuning the ratio between Dextran and Alginate and the concentration of dendrimer we generated a material platform with a broad range of properties with gelation times

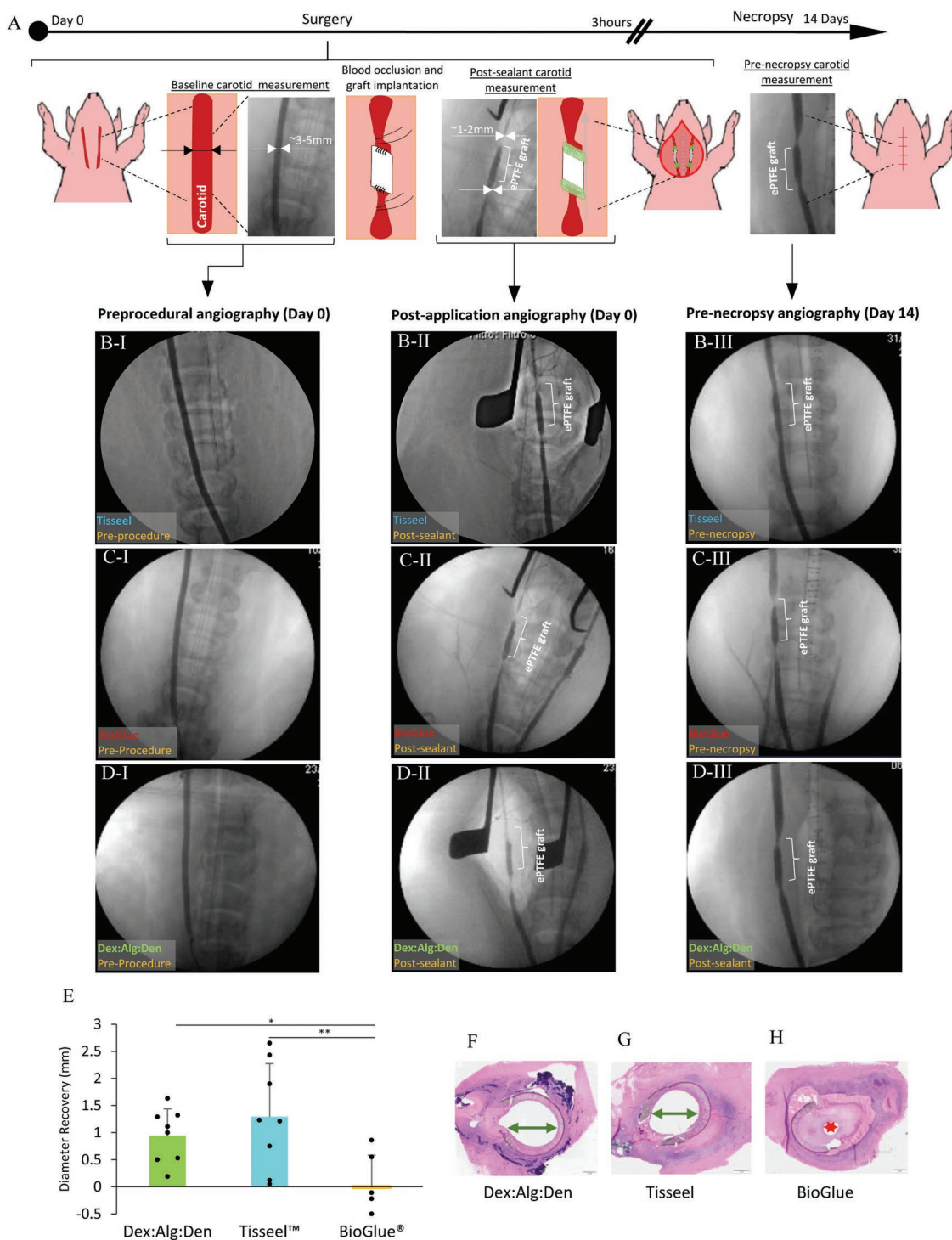


Figure 9. Evaluation of bilateral carotid vascular graft followed by suture line sealing with vascular sealants in a porcine model. A) Description of the procedure and timeline. B-I, C-I, D-I) Angiography was performed pre-procedure to measure the diameter of the carotids to inform the choice of graft diameter for Tisseel, BioGlue, and 15%Dex:5%Alg:30%Den, respectively. B-II, C-II, D-II) Right after sealant application, a second angiography was taken to have a measurement of the narrowed vessel following blood occlusion for Tisseel, BioGlue, and Dex:Alg:Den, respectively. B-III, C-III, D-III) A final angiography was taken prior to necropsy to study vessel recovery following material application at day 14 for Tisseel, BioGlue, and 15%Dex:5%Alg:30%Den, respectively. E) The final vessel diameter at necropsy was measured using quantitative vascular analysis. Both 15%Dex:5%Alg:30%Den and Tisseel displayed a positive recovery over the 14-d period, while BioGlue displayed no recovery or even some contraction during the same period, Dex:Alg:Den $n = 12$, Tisseel $n = 8$, and BioGlue $n = 6$. F–H) Representative images of the H&E staining for the three materials at day 14, both 15%Dex:5%Alg:30%Den (F) and Tisseel (G) display open lumen, while BioGlue (H) displays an excessive neointima formation. Data are presented as mean \pm SD. P -values are calculated using two-sided t -test. * $P < 0.05$, ** $P \leq 0.01$, *** $P \leq 0.001$. Scale bar = 1 mm.

ranging from 5 to 160 s, degradation times within 1 d to more than one month, and compressive strengths from 50 to 750 kPa.

We also demonstrated the compatibility of Dex:Alg:Den sealant with industrial sterilization methods (20 kGy gamma irradiation) with no loss of efficacy or biocompatibility and the sprayability using a non-air-assisted spray. These properties are of critical importance as many emerging materials degrade upon gamma irradiation and may require specific applicators. While the gold-standard criteria for material biocompatibility is cell viability above 70% in the NRU test, Dex:Alg:Den sealant displayed values well above 90%. While often ignored in the early development stages, sensitization and genotoxicity studies are a critical requisite to advance in the clinical translation of any material. We demonstrated that Dex:Alg:Den materials are not genotoxic and do not cause any sign of allergic reaction or sensitization.

We validated material safety and efficacy in vitro, ex vivo, and in large animal models. A suprathreshold burst pressure of an average of 300 mmHg using the graft-carotid model was achieved, which would be enough to withstand hypertensive patients and it is well above the nonpathological blood pressure of 80–120 mmHg. We chose a carotid-ePTFE graft anastomosis as a very challenging model in which the material is required to maintain strong interaction both with the biological tissue and prosthetic material. Dex:Alg:Den displayed superior overall performance lacking any type of adverse event. We used BioGlue and Tisseel as control materials, two well-characterized commercial materials that represent strong adhesion and adequate biocompatibility, respectively. Some of the adverse events that we saw, were aligned with the literature and with clinically documented drawbacks of these materials.^[19,36] In the swine study, one of the Tisseel treated animals, which is known to display limited adhesion, experienced severe bleeding post-surgery that required an emergency procedure. In the rabbit study, one of the animals had to be euthanized because of the constriction caused by the BioGlue when applied in the aorta. When using the BioGlue in the pigs, one of the carotids was fully occluded after 14 d, which further reinforces the concern of dangerous side effects.

Emerging materials such as poly(glycerol-sebacate) acrylate (PGSA) commercialized by Tissium have demonstrated how new approaches are able to beat traditional materials. In a preclinical and clinical setup it has been demonstrated that this light activated material mechanically interlocks with the tissue surface, resulting in superior performance to that of BioGlue,^[31,37] with the latter leading to vessel narrowing and neointima formation (similarly to our findings here). Yet, the need to use light to trigger the gelation of the material can hinder its clinical adoption since the same material can provide different or heterogeneous properties depending on the length of the light activation step.

The suboptimal performance of traditional sealants highlights the need for next-generation solutions. The use of multiple mechanisms such as ionic interactions, or mechanical interlocking with tissue and prosthetic surfaces stands as a superior approach to improving clinical outcomes while limiting complications. Yet, these new materials should ideally spontaneously gel to enable rapid and easy application by clinicians. Gelation time as well as the rheological properties of

the material would also determine the precision by which the material can be applied to the target site. The aforementioned design considerations become even more critical with the steady shift of the traditional surgeries into minimally invasive procedures, in which the usability of most clinically approved materials is very limited. The strategy used herein to create high-pressure-resistant sealants was validated in a challenging preclinical vascular model and has the potential to be applied to other indications where surgical sealants could greatly improve patient clinical outcomes such as in dura sealing, gastrointestinal applications, and nerve repair among others.

4. Conclusions

We report on a new hydrogel adhesive platform based on polyaldehyde component (composed of oxidized dextran and oxidized alginate) and a PAMAM dendrimer component that achieves suprathreshold burst pressures while the highest standards of biocompatibility following FDA guided studies that has been facilitated by combining covalent and non-covalent bonds to improve adhesion. This versatile and functional platform, formed by the competitive internal interaction between the polymers and their external interactions with the tissue, can provide a broad range of material mechanical and biological properties. We sought to use challenging preclinical conditions to test the potential translation of this material to the clinic and hence tested our material's performance in the conventional model of vessel puncture, as well as in ePTFE graft carotid vascular reconstruction followed by anticoagulant and antiaggregant dual therapy which is routinely used in patients and where clinicians struggle to find adequate biomaterial-based solutions. The combination of robust biocompatibility assays in cell culture, guinea pigs and rabbits, as well as rigorous functional studies in rabbits and pigs provide comprehensive assessment of material performance under clinically relevant conditions.

5. Experimental Section

Synthesis of Oxidized Polysaccharides: Aldehydes were introduced in the polysaccharides using sodium periodate oxidation as previously described.^[38] First, 19.6 g of dextran were dissolved in 160 mL of deionized water. In parallel, 17.8 g of sodium periodate were dissolved in 170 mL of deionized water and added slowly to the dextran solution under continuous stirring. After 5 h the oxidized polymer was transferred to 3.5 kDa cutoff dialysis membranes (3.5 kD molecular weight cutoff (MWCO) Repligen) and dialyzed for 4 d with daily changes of water. The purified polysaccharide was then frozen to -80°C and lyophilized until dry. Alginate oxidation was performed in a 1:1 mixture of deionized water:ethanol. 10 g of alginate were dispersed in 150 mL of water:ethanol solution and 5 g of NaIO_4 dissolved in 150 mL of water was slowly added to the mixture while stirred. After 4 h the oxidized alginate was transferred to 3.5 kDa dialysis membranes and the water was renewed twice a day for 4 d. Then it was frozen to -80°C and lyophilized until dry. Chemical modification of oxidized dextran and oxidized alginate was confirmed by FTIR spectroscopy.

Hydrogel Stability: To study the hydrogel stability, the swelling, water content, and gel fraction were studied. To calculate the swelling, hydrogels were created by mixing 100 μL of the polysaccharide component with 100 μL of PAMAM dendrimer. Then hydrogels were

immediately moved into a 24-well plate with 500 μL of 1 \times PBS per well. The sealed plate was then placed in a 37 $^{\circ}\text{C}$ incubator at 200 rpm. The swelling was then calculated at 6 and 24 h as follows: Swelling (%) = $(w_s - w_i)/w_i$, where w_s is the wet mass of the hydrogel and w_i is the initial wet mass of the hydrogel at time 0. To calculate the water content, the hydrogel discs were rinsed with distilled water for 15 min to remove the 1 \times PBS salts and then lyophilized overnight. Water content was calculated using the following formula Water content (%) = $(w_s - w_{\text{dry}})/w_s$, where w_{dry} is the mass of the dry polymer after lyophilization. To calculate the gel fraction, the following formula was used: Gel fraction (%) = $w_{\text{dry}}/w_{i,\text{dry}}$. To obtain $w_{i,\text{dry}}$ the hydrogel components were allowed to crosslink for 5 min, then rinsed with distilled water to eliminate potential unreacted polymer chains and then lyophilized overnight to obtain the dry mass.

Compressive Strength: Gels were created by mixing 100 μL of the polysaccharide component with 100 μL of PAMAM dendrimer. After 5 min allowing the crosslinking reaction to occur, the gels were tested under compression (Instron Tensile Tester 5942) at a rate of 0.05 mm s^{-1} and the stress at break was measured.

Viscosity Measurements: 400 μL of polymer solution were loaded in a H-100-2 Viscometer pipette, then loaded into the RheoSense microVISC. The temperature was not controlled but room temperature was maintained at 22 $^{\circ}\text{C}$. Three consecutive measurements were performed for each solution.

Burst Pressure: Freshly harvest swine intestine was cut into pieces of 2.5 $\text{cm} \times 2.5 \text{ cm}$. A 3 mm hole was performed in the center of the specimen. The tissue was then placed in the tissue holder and fixed. A single suture point was added to approximate the edges of the hole, yet without holding any pressure. About 200 μL of sealant were delivered on top of the tissue. After 5 min the pressure was increased in the circuit by a syringe pump at 10 mL min^{-1} . The pressure was measured by a PendoTECH pressure sensor. The maximum pressure at bursting was measured as burst pressure.

To evaluate the performance of the adhesive in the actual ePTFE graft–carotid interface, a freshly harvested pig carotid was sutured ex vivo to a 4 mm diameter ePTFE vascular graft. The loose end of the graft was clamped while the nongrafted end of the carotid was connected to the circuit with the pressure sensor and the syringe pump.

Fluorescent Labeling of the Material: To monitor the material degradation pre- and post-gamma irradiation, the different polymers were tagged fluorescently. The materials were tagged after gamma irradiation to avoid potential modifications on the fluorescent molecules caused by the radiation. Both oxidized dextran (Alexa Fluor-488) and oxidized alginate (Alexa Fluor-594) were modified as follows. 5 mg of oxidized polysaccharide were dissolved in 0.5 mL of 50×10^{-3} M sodium bicarbonate buffer (pH 8.5). 1 mg of Alexa Fluor 488 or 594 hydrazide (Thermo Fisher) was dissolved in 300 μL of sodium bicarbonate buffer (pH 8.5) and added dropwise to the stirring polysaccharide solution and allowed to react for 1 h. Then, the reaction mix was cooled down in an ice-water bath and 0.5 mL of 30×10^{-3} M sodium cyanoborohydride solution were added and allowed to react for 3 h. To eliminate unreacted fluorescent molecules and salts, the reaction mix was dialyzed through a 3000 Da MWCO centrifugal filter (Amicon Ultra-15, EMD Millipore) against deionized water. The resulting solution was lyophilized until dry.

PAMAM dendrimer was tagged following a similar protocol. 3 mg of G5 PAMAM dendrimer (75% OH, 25% NH_2) were diluted to a concentration of 1% $_{w/w}$ in 0.1 M sodium bicarbonate buffer (8.3). 0.1 mg of Alexa Fluor 647-NHS were dissolved in 0.1 mL of DMSO. While stirring the dendrimer solution, the dye solution was added slowly. After 1 h of reaction at room temperature, the reaction mixture was dialyzed using deionized water using a 3000 Da MWCO centrifugal filter (Amicon Ultra-15, EMD Millipore). The resulting solution was lyophilized until dry.

Gelation Time: Gelation time was measured pre and post-sterilization of the material to assess any potential impact due to the gamma radiation. 100 μL of each component was mixed in an inverted cap of a 1.5 mL Eppendorf tube containing a magnetic stirring bar. The material fully gelled was considered when the stirring bar stops the rotation. As the Dex:Alg:Den formulation is designed to achieve an instant gelation, any potential difference in gelation would be too small to be measured

with this method. To maximize the potential differences in the gelation profile of the material after being irradiated, the same experiment was conducted but using a water diluted formulation in a ratio 1:3, 33 μL of each component were diluted with 66 μL of water to generate a final formulation of 5% dextran, 1% alginate, and 10% dendrimer. The diluted formulations allowed much longer gelation times providing with enough resolution to identify potential changes.

Degradation Study: The aim of this study is to understand if there is any change in the degradation profile of the bulk material after being gamma irradiated. The degradation of materials from the same synthesis batch was compared before and after being treated with a dose of 20 kGy. To track the material degradation, each one of the sealant components (dendrimer, dextran, and alginate) was tagged fluorescently with different fluorophores. Each disc, 100 μL size, was prepared by mixing 50 μL of polysaccharide solution with 50 μL of dendrimer solution, the mixed solution was placed in a cylindrical mold of 5 mm diameter and ≈ 4 mm height. Precast discs were placed in a 24-well plate and stirred at 250 rpm and 37 $^{\circ}\text{C}$ in 500 μL of 1 \times PBS which was replaced every day for one week and then every other day till day 30.

The 500 μL collected for each one of the samples were used to analyze the amount of fluorescent material released (degraded from the material) for that timeframe. To measure the fluorescence, a SpectraMax i3x plate reader from Molecular Devices was used. The total amount of fluorescent material in each sealant disc is known, thus allowing a facile conversion between fluorescence and degradation (wt%). Each group contains nine replicates.

In Vitro Cell Viability: All the in vitro cell viability studies were performed following the FDA recommendations for evaluation of safety of medical devices gathered on the ISO 10993-5. The NRU test consisted in the assessment of the viability of L929 mouse fibroblast after the exposure to sealant extracted media or individual components. All the materials tested were sterilized using a 0.2 μm filter (ePTFE, 0.2 μm , 13 mm Cytiva Whatman Uniflo Syringe Filters).

To evaluate the cell toxicity created by the individual components, different amounts of the polymers were dissolved in DMEM containing 10% FBS and 200 μL directly applied on top of a 70%–80% confluent L929 mouse fibroblast. The plate was incubated for 24 h at 37 $^{\circ}\text{C}$ under sterile conditions. Negative controls to account for 100% viability were created by using 10% FBS DMEM media without any polymer. Then, the polymer containing media was removed and substituted by 100 μL of neutral red containing media (40 $\mu\text{g mL}^{-1}$). Cells were again incubated for 2 h in which the viable cells will incorporate the neutral red dye into their lysosomes. After the incubation period, the well plates are immersed in PBS to completely remove the neutral red containing media. To extract and dissolve the dye incorporated by the cells, 150 μL of distain solution composed by 50% ethanol, 49% deionized water, and 1% glacial acetic acid. The OD of the neutral red extract was then measured at 540 nm using the SpectraMax i3x plate reader from Molecular Devices.

To evaluate the cell toxicity of specific sealant formulations, 1 mL (≈ 1 g) of sealant was cast in a sterile cylindrical mold and placed in a 15 mL conical tube with 5 mL of 10% FBS DMEM media. The sealant was incubated in the shaker for 24 h at 250 rpm and 37 $^{\circ}\text{C}$. Then, the treated media was applied into 70%–80% confluent L929 mouse fibroblast and incubated for 24 h. Negative controls to account for 100% viability were created by using 10% FBS DMEM media. The neutral red incubation and distain steps were performed following the same protocol explained above.

Reverse Mutation Ames Genotoxicity: This assay was used to detect reverse mutations within the histidine or tryptophan operon which are analyzed in the form of induction of histidine independent growth (*S. typhimurium*) or tryptophan independent growth (*Escherichia coli*). The sealant was extracted in a polar (NaCl) and a nonpolar (DMSO) vehicle at 50 $^{\circ}\text{C}$ for 72 h. The different bacteria strains were exposed to this extract via plate incorporation, in the presence or absence of metabolic activation. The number of colonies after 48 h of incubation at 37 $^{\circ}\text{C}$ will indicate the mutagenic potential of the material extract. For each strain and condition, the numbers of colonies after exposure to the test article are compared to those of a negative control. The test article

is considered not mutagenic if the difference is found not statistically significant ($p > 0.05$) to the negative control.

Guinea Pig Sensitization: The purpose of the Kligman sensitization study is to determine the potential allergenic or sensitizing capacity of the Dex:Alg:Den sealants. The study was conducted based upon the ISO 10993-10, Biological Evaluation of Medical Devices, part 10: Test for irritation and Skin Sensitization. Hartley Guinea pigs, 20 experimental, 10 negative control, and 5 positive controls, were used for this study. 5% Dinitrochlorobenzene (DNCEB) in 95%EtOH was used as positive control and saline was used as negative control. Dex:Alg:Den sealant was extracted at 0.2 g mL⁻¹ in polar (USP 0.9% sodium chloride for injection) and nonpolar (cottonseed Oil "CSO") for 24 h at 70 °C. Polar extraction mimics the body conditions to extract leachables that would be released from the sealant in polar environment. The nonpolar extraction, using CSO, mimics the leachable that will be released from the sealant in nonpolar body tissues as fat. The study began with an induction phase (Day 0) where the sealant extract and controls were injected intradermally. The topical application phase (say 7) was conducted by applying the sealant extract or control for 48 h, at the site of the intradermal injections. On day 23 the challenge phase is performed by topically applying the extract and grading the erythema and edema at 24, 48, and 71 h post challenge application. This study was performed by Toxikon Inc., following standard procedure and animal care and welfare standards ISO10993-2 2006 and AAALAC.

Rabbit Subcutaneous Implantation: This study consisted of three groups of four female New Zealand white rabbits. All animals underwent a surgical procedure on day 0 in which six subcutaneous pockets were created, three on each side of the spine. Dex:Alg:Den and control materials were prepared according to the manufacturer's instructions and injected directly into the pocket at a volume of ≈0.5–1 mL per pocket. At 7, 14, and 30 d animals were euthanized and implant sites as well as evidence of macroscopic findings were collected into 10% formalin for histomorphology evaluation by a professional pathologist. Implant sites samples were paraffin processed and sectioned lengthwise to create slides, which were stained with hematoxylin and eosin (H&E) and Masson's trichrome (MT). This study was performed by CBSET INC, accredited by AAALAC International, IACUC Project Number: I00231.

Rabbit Aorta Puncture Model: This study consisted of three groups with a total of 17 female New Zealand white rabbits, six in the Dex:Alg:Den and Tisseel group, and five in the BioGlue. An incision was performed along the midline abdomen. Once through the skin, blunt and sharp dissection was used to access the linea alba. The linea was then incised to access the peritoneal cavity. The aorta (below the renal arteries to guarantee vascular supply to abdominal organs) was isolated via blunt dissection. Proximal and distal regions of the aorta were occluded using umbilical tape. Heparin (1000U, IV) was administered prior to occlusion. A 21-G needle (external diameter 0.8192 mm) was used to puncture the aorta. At the puncture location aorta diameter was around 2–3 mm. Bleeding at the puncture sites was visually confirmed and then treated with Dex:Alg:Den Sealants or Control devices. Sealants were allowed to cure for the appropriate duration (up to 5 min) prior to restoring blood flow. This study was performed by CBSET INC, accredited by AAALAC International, IACUC Project Number: I00231.

Swine Bilateral Carotid Graft Placement: The study consisted of seven Yorkshire pigs, three for the Dex:Alg:Den group, and two for each one of the controls, Tisseel and BioGlue. Each graft placed provided two suture lines (distal & proximal) where sealing had to be achieved. The total number of tissue:graft interfaces to be sealed was 12 for Dex:Alg:Den, and 8 for Tisseel and BioGlue. The procedure consisted a porcine model in which both carotids undergo a graft placement, the diameter of the vessels was between 4 and 6 mm in diameter. Animals underwent bilateral carotid graft implantation followed by the application of the tested sealant. The carotid artery was prepared and an appropriately sized vascular ePTFE graft was cut to a target angle of 45° (or similar) to produce a lumen of approximately similar size as the arteriotomy. The graft was anastomosed to the arteriotomy in an end-to-side fashion. The suture lines were treated with the test or control sealant, as appropriate to the group and devices were allowed to cure for

the appropriate duration (up to 5 minutes) prior to restoring blood flow. The procedure was repeated for the contralateral artery using the same test device. Each animal was treated with only one test or control device. Activated clotting times (ACT) were monitored during the procedure and maintained high enough to avoid any thrombus formation during the procedure. Aspirin and clopidogrel were administered daily for antiplatelet therapy. This study was performed by CBSET INC, accredited by AAALAC International, IACUC project number I00263.

Quantitative Vascular Analysis: Fluoroscopy was used to qualitatively evaluate the carotid artery at the region of the graft. Angiographic quantitative vascular analysis (QVA) was performed before starting the procedure, post-treatment and before necropsy. The quantitative vascular analysis values were obtained using the Centricity Cardiology CA1000 Cardiac Review 2.0 software. The vessel recovery was measured comparing the diameter post-treatment and pre-necropsy.

Statistical Analysis: Microsoft Excel was used to evaluate statistical significance of results in this work. In the statistical analysis between two groups, a two-sample Student's *t*-test was used, the significance level was placed at * $p \leq 0.05$, ** $p \leq 0.01$, and *** $p \leq 0.001$.

Supporting Information

Supporting Information is available from the Wiley Online Library or from the author.

Conflict of Interest

N.A. and E.R.E. are co-founders of BioDevek Inc. which holds patents on the described materials.

Data Availability Statement

The data that support the findings of this study are available from the corresponding author upon reasonable request.

Keywords

adhesive hydrogels, surgical sealants, translational research

Received: April 5, 2022
Revised: August 11, 2022
Published online: October 3, 2022

- [1] M. E. Stokes, X. Ye, M. Shah, K. Mercaldi, M. W. Reynolds, M. F. T. Rupnow, J. Hammond, *BMC Health Serv. Res.* **2011**, *11*, 135.
- [2] A. Shander, *Surgery* **2007**, *142*, 20.
- [3] A. B. Lumsden, E. R. Heyman, *J. Vascul. Surg.* **2006**, *44*, 1002.
- [4] N. Belkin, J. B. Stoecker, B. M. Jackson, S. M. Damrauer, J. Glaser, V. Kalapatapu, M. A. Golden, G. J. Wang, *J. Vascul. Surg.* **2021**, 930.
- [5] S. Nam, D. Mooney, *Chem. Rev.* **2021**, 11336.
- [6] G. M. Taboada, K. Yang, M. J. N. Pereira, S. S. Liu, Y. Hu, J. M. Karp, N. Artzi, Y. Lee, *Nat. Rev. Mater.* **2020**, *5*, 310.
- [7] H.-H. Chao, D. F. Torchiana, *J. Card. Surg.* **2003**, *18*, 500.
- [8] W. G. Schenk III, W. D. Spotnitz, S. G. Burks, P. H. Lin, R. L. Bush, A. B. Lumsden, *Am. Surg.* **2005**, *71*, 658.
- [9] W. Fürst, A. Banerjee, *Ann. Thorac. Surg.* **2005**, *79*, 1522.
- [10] P. A. Leggat, D. R. Smith, U. Kedjarune, *ANZ J. Surg.* **2007**, *77*, 209.
- [11] J. Yang, R. Bai, B. Chen, Z. Suo, *Adv. Funct. Mater.* **2020**, *30*, 1901693.
- [12] Y. Liu, W. He, Z. Zhang, B. Lee, *Gels* **2018**, *4*, 46.

- [13] M. Mehdizadeh, H. Weng, D. Gyawali, L. Tang, J. Yang, *Biomaterials* **2012**, *33*, 7972.
- [14] J. Li, A. D. Celiz, J. Yang, Q. Yang, I. Wamala, W. Whyte, B. R. Seo, N. V. Vasilyev, J. J. Vlassak, Z. Suo, D. J. Mooney, *Science* **2017**, *357*, 378.
- [15] S. J. Wu, H. Yuk, J. Wu, C. S. Nabzdyk, X. Zhao, *Adv. Mater.* **2021**, *33*, 2007667.
- [16] M. H. Murdock, J. T. Chang, S. K. Luketich, D. Pedersen, G. S. Hussey, A. D. Amore, S. F. Badylak, *J. Thorac. Cardiovasc. Surg.* **2019**, *157*, 176.
- [17] N. Oliva, M. Carcole, M. Beckerman, S. Seliktar, A. Hayward, J. Stanley, N. M. A. Parry, E. R. Edelman, N. Artzi, *Sci. Transl. Med.* **2015**, *7*, 272ra11.
- [18] J. Conde, N. Oliva, Y. Zhang, N. Artzi, *Nat. Mater.* **2016**, *15*, 1128.
- [19] A. C. Rogers, L. P. Turley, K. S. Cross, M. P. McMonagle, *Br. J. Surg.* **2016**, *103*, 1758.
- [20] P. Sergeant, R. Kocharian, B. Patel, M. Pfefferkorn, J. Matonick, *Interact. Cardiovasc. Thorac. Surg.* **2016**, *22*, 813.
- [21] A. Jejurikar, X. T. Seow, G. Lawrie, D. Martin, A. Jayakrishnan, L. Grøndahl, *J. Mater. Chem.* **2012**, *22*, 9751.
- [22] R. G. Huamani-Palomino, B. M. Córdova, L. E. Renzo Pichilingue, T. Venâncio, A. C. Valderrama, *Polymers* **2021**, *13*, 255.
- [23] D. Kedarla, R. Vasita, *J. Tissue Eng.* **2017**, *8*, <https://doi.org/10.1177/204173141771839>.
- [24] S. Materials, *Annual Book of ASTM Standards*, ASTM International, West Conshohocken, PA, USA **2011**, <https://doi.org/10.1520/F2392-04R15>.
- [25] G. Repetto, A. del Peso, J. L. Zurita, *Nat. Protoc.* **2008**, *3*, 1125.
- [26] S. Pourshahrestani, E. Zeimaran, N. A. Kadri, N. Mutlu, A. R. Boccaccini, *Adv. Healthcare Mater.* **2020**, *9*, 2000905.
- [27] C. Ghobril, M. W. Grinstaff, *Chem. Soc. Rev.* **2015**, *44*, 1820.
- [28] L. Han, X. Lu, K. Liu, K. Wang, L. Fang, L. T. Weng, H. Zhang, Y. Tang, F. Ren, C. Zhao, G. Sun, R. Liang, Z. Li, *ACS Nano* **2017**, *11*, 2561.
- [29] C. Fan, J. Fu, W. Zhu, D. A. Wang, *Acta Biomater.* **2016**, *33*, 51.
- [30] C. E. Brubaker, H. Kissler, L. J. Wang, D. B. Kaufman, P. B. Messersmith, *Biomaterials* **2010**, *31*, 420.
- [31] D. Wussler, S. Kiefer, S. Naumann, D. Hackner, J. Nadjiri, S. Meckel, J. Haberstroh, R. Kubicki, A. Seifert, M. Siepe, P. Ewert, B. Stillner, N. Lang, *Interact. Cardiovasc. Thorac. Surg.* **2020**, *30*, 715.
- [32] X. Xu, X. Xia, K. Zhang, A. Rai, Z. Li, P. Zhao, K. Wei, L. Zou, B. Yang, W. K. Wong, P. W. Y. Chiu, L. Bian, *Sci. Transl. Med.* **2020**, *12*, eaba8014.
- [33] H. Yuk, C. E. Varela, C. S. Nabzdyk, X. Mao, R. F. Padera, E. T. Roche, X. Zhao, *Nature* **2019**, *575*, 169.
- [34] T. Zhang, H. Yuk, S. Lin, G. A. Parada, X. Zhao, *Acta Mech. Sin.* **2017**, *33*, 543.
- [35] X. Zhao, *Soft Matter* **2014**, *10*, 672.
- [36] S. A. LeMaire, Z. C. Schmittling, J. S. Coselli, A. Ündar, B. A. Deady, F. J. Clubb, C. D. Fraser, *Ann. Thorac. Surg.* **2002**, *73*, 1500.
- [37] Q. Pellenc, J. Touma, R. Coscas, G. Edorh, M. Pereira, J. Karp, Y. Castier, P. Desgranges, J. M. Alsac, *J. Cardiovasc. Surg.* **2019**, *60*, 599.
- [38] N. Oliva, S. Shitreet, E. Abraham, B. Stanley, E. R. Edelman, N. Artzi, *Langmuir* **2012**, *28*, 15402.